CONVEX POLYTOPES FROM NESTED POSETS

SATYAN L. DEVADOSS, STEFAN FORCEY, STEPHEN REISDORF, AND PATRICK SHOWERS

Abstract. Motivated by the graph associahedron $\mathcal{K}G$, a polytope whose face poset is based on connected subgraphs of G, we consider the notion of associativity and tubes on posets. This leads to a new family of simple convex polytopes obtained by iterated truncations. These generalize graph associahedra and nestohedra, even encompassing notions of nestings on CW-complexes. However, these *poset associahedra* fall in a different category altogether than generalized permutohedra.

1. Background

1.1. Given a finite graph G, the graph associahedron $\mathcal{K}G$ is a polytope whose face poset is based on the connected subgraphs of G [4]. For special examples of graphs, $\mathcal{K}G$ becomes well-known, sometimes classical: when G is a path, a cycle, or a complete graph, $\mathcal{K}G$ results in the associahedron, cyclohedron, and permutohedron, respectively. Figure 1 shows some examples, for a graph and a pseudograph with multiple edges. These polytopes were

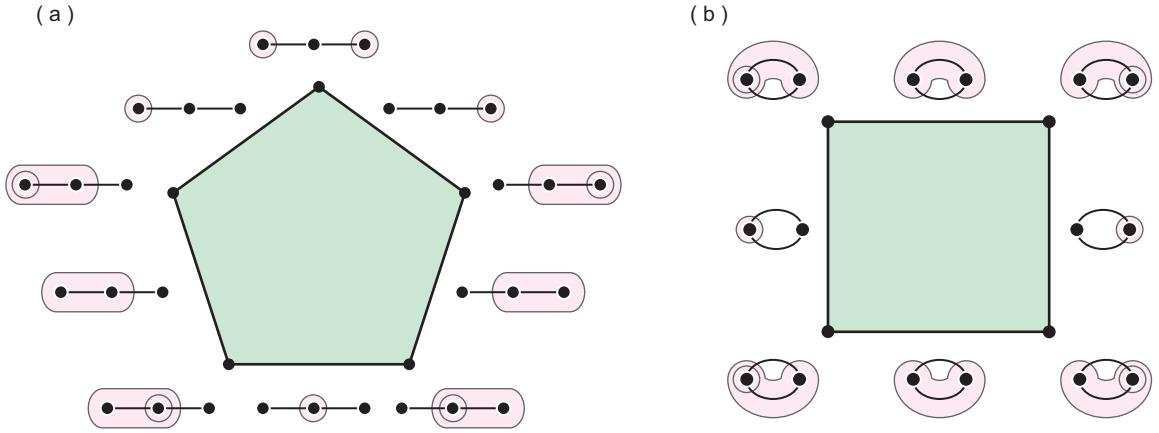

Figure 1. Graph associahedra of a path and a multi-edge.

first motivated by De Concini and Procesi in their work on 'wonderful' compactifications of hyperplane arrangements [6]. In particular, if the hyperplane arrangement is associated to a Coxeter system, graph associahedra $\mathcal{K}G$ appear as tilings of the 'minimal' compactification of these spaces, where its underlying graph G is the Coxeter graph of the system

2000 *Mathematics Subject Classification.* Primary 52B11, Secondary 55P48, 18D50.
Key words and phrases. poset, graph associahedron, nesting, polytope.

[5]. These compactified arrangements are themselves natural generalizations of the Deligne-Knudsen-Mumford compactification $\overline{\mathcal{M}}_{0,n}(\mathbb{R})$ of the real moduli space of curves [7]. From a combinatorics viewpoint, graph associahedra arise in numerous areas, ranging from Bergman complexes of oriented matroids to Heegaard Floer homology [1]. Most notably, these polytopes have emerged as graphical tests on ordinal data in biological statistics [12].

1.2. Motivated by De Concini and Procesi, Feichtner and Kozlov [10] generalized the definition of building and nested sets to the combinatorial case. Since these structures expose the fundamental concepts of connectivity, it is not surprising that there have been several extensions [13, 14, 18]. However, none of these constructions capture the notion of nested sets of posets, as we do below. Indeed, our notion of the set of poset tubes is not a classical building set, but falls in a different category altogether.

In this paper, we construct a new family of convex polytopes which are extensions of nestohedra and graph associahedra via a generalization of building sets. Rather than starting with a set, we begin with a poset P and its connected lower sets, resulting in the *poset associahedron* $\mathcal{K}P$. It is combinatorially equivalent to a wide swath of existing examples from geometric combinatorics, including permutohedra, associahedra, multiplihedra, graph associahedra, nestohedra, pseudograph associahedra, and their liftings; in fact, all these types are just from rank two posets. Newly discovered are polytopes capturing associativity information of CW-complexes.

An overview of the paper is as follows: Section 2 supplies the definitions of poset associahedra along with several examples, while Section 3 provides methods of constructing them via truncation. Specialization to nestohedra and permutohedra is given in Section 4, and we finish with proofs of the main theorems in Section 5.

2. Posets

2.1. We begin with some foundational definitions about posets. The reader is forewarned that definitions here might not exactly match those from earlier works. A *lower set* L is a subset of a poset P such that if $y \preceq x \in L$, then $y \in L$. A subset of P is *connected* if the Hasse diagram of the subset is connected as a graph. The *boundary* of an element x is $\partial x := \{y \in P \mid y \prec x\}$.

Definition. The *bundle* of element x is the set $\mathfrak{b}_x := \{y \in P \mid \partial y = \partial x\}$. A bundle is *singleton* if $\mathfrak{b}_x = \{x\}$.

Throughout this paper, a poset will be visually represented by its Hasse diagram. Consider the example of a poset P given on the left side of Figure 2. The subset $\{1, 2, 4, 5\}$ in part (a), depicted by the highlighted region, is not a lower set since it does not include element 3.

This poset is partitioned into four bundles, $\mathfrak{b}_1 = \mathfrak{b}_2 = \mathfrak{b}_3 = \{1, 2, 3\}$, $\mathfrak{b}_4 = \{4\}$, $\mathfrak{b}_5 = \{5\}$, and $\mathfrak{b}_6 = \mathfrak{b}_7 = \mathfrak{b}_8 = \{6, 7, 8\}$, with elements in a bundle having identical boundary. In particular, notice that all minimal elements of the poset are in one bundle since they share the empty set as boundary; we call this bundle the *minimal* bundle. The following is immediate:

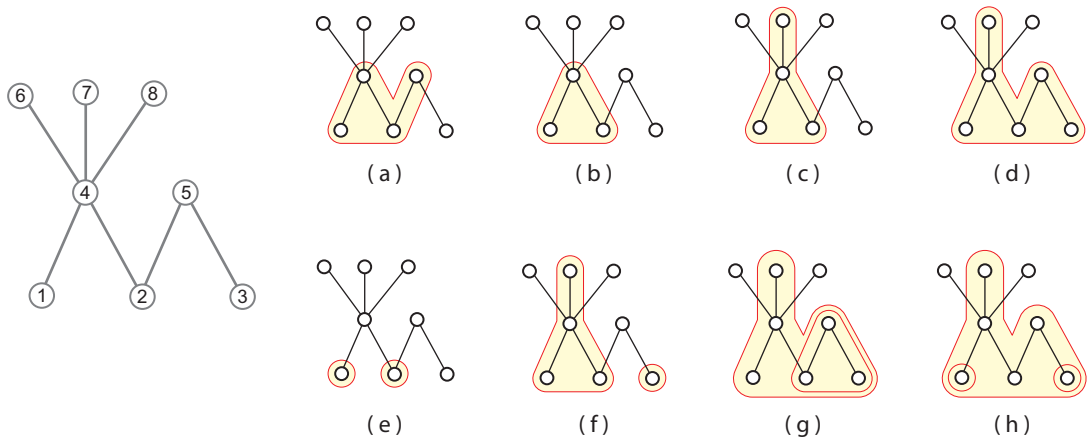

FIGURE 2. Some examples of valid and invalid tubes and tubings.

Lemma 1. *The elements of poset P are partitioned into equivalence classes of bundles.*

Definition. A lower set is *filled* if, whenever it contains the boundary ∂x of an element x, it also intersects the bundle $\mathfrak{b}_x$ of that element. A *tube* is a filled, connected lower set. A *tubing* T is a collection of tubes (not containing all of P) which are pairwise disjoint or pairwise nested, and for which the union of every subset of T is filled.

Figure 2(b) shows the boundary of $\{6, 7, 8\}$, which is an unfilled lower set, whereas (c) is a filled one. Note that parts (c, d) display examples of one tube. Parts (e, f) display two disjoint tubes which are not tubings, since the union of the tubes would create an unfilled lower set. Examples of tubings with two and three components are given by (g, h) respectively.

2.2. We now present our main result.

Theorem 2. *Let P be a poset with n elements partitioned into b bundles. Define $\pi(P)$ to be the set of tubings partially ordered by reverse containment. There exists a convex polytope of dimension $n - b$, the* poset associahedron *$\mathcal{K}P$, whose face poset is isomorphic to $\pi(P)$.*

This result follows from the construction of $\mathcal{K}P$ from truncations, described in Theorem 6 below. The following allows us to consider only connected posets, where Δ_k denotes the simplex of dimension k:

Proposition 3. *Let P be a poset with connected Hasse components $P_1, \ldots, P_m$. Then $\mathcal{K}P$ is isomorphic to $\mathcal{K}P_1 \times \cdots \times \mathcal{K}P_m \times \Delta_{m-1}$.*

Proof. Any tubing of P can be described as:

(1) a listing of tubings $T_1 \in \mathcal{K}P_1, \ \ldots, \ T_m \in \mathcal{K}P_m$, and
(2) for each component P_i either including or excluding the tube $T_i = P_i$, as long as all tubes P_i are not included.

The second part of this description is clearly isomorphic to a tubing of the edgeless graph H_m on m nodes. But from [8, Section 3], since $\mathcal{K}H_m$ is the simplex Δ_{m-1}, we are done. □

Example. Figure 3 shows the two polytopes of Figure 1, reinterpreted as tubings on posets of their underlying graphs. Both posets have *rank two*, the number of elements in any maximal chain of the poset. Part (a) has 5 elements and 3 bundles, whereas (b) has 4 elements and 2 bundles, both resulting in polygons, as given in Theorem 2.

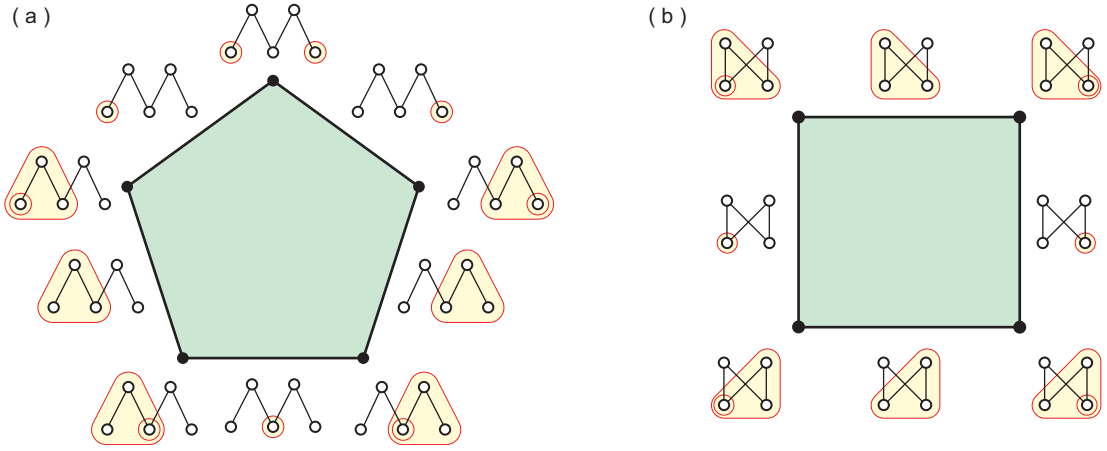

FIGURE 3. Poset versions of Figure 1.

Example. Figure 4 shows two different posets, resulting in identical poset associahedra as Figure 3. Part (a) shows a poset structure which does not even come from a CW-complex. Notice here that the left element of height zero cannot be a tube since it needs to be filled. Part (b) has a near identical structure to Figure 3(b). Here, the bottom-right element cannot be a tube in itself since it is unfilled. Because both posets have 5 elements and 3 bundles, the dimension of the polytopes is two.

In certain situations, such as Figures 3(b) and 4(b), altering the underlying poset does not affect the polytope. This can be presented formally:

Proposition 4. *Let x be a maximal element of a maximal chain of P such that $\mathfrak{b}_x$ is a singleton bundle. If ∂x is connected, then $\mathcal{K}P = \mathcal{K}(P - x)$.*

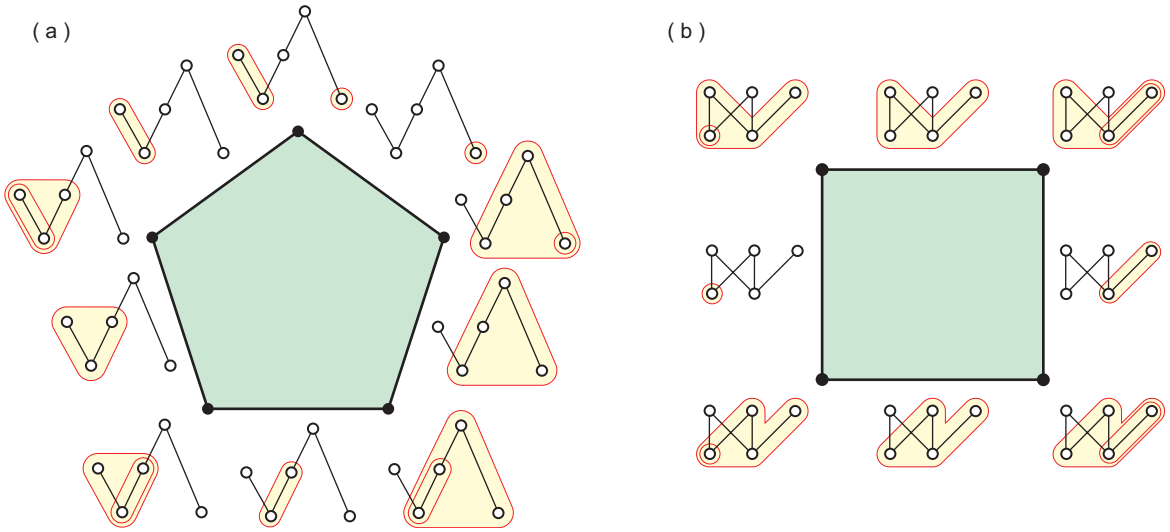

FIGURE 4. Alternate poset associahedra.

Proof. We show that t is a tube of P if and only if $t - x$ is a tube of $P - x$. If $x \notin t$, then $\partial x \notin t$, and t has the properties of a tube in both P and $P - x$, or in neither. On the other hand, if $x \in t$, then $\partial x \in t$, and so t is connected if and only if $t - x$ is connected. Extending this isomorphism of tubes to tubings preserves this containment. □

Example. Three examples of 3D poset associahedra are given in Figure 5. The cube in (a) can be viewed as an extension of the square in Figure 3(b), and Proposition 14 generalizes this pattern to the n-cube. Note that both (a) and (b) are posets with 6 elements partitioned into 3 bundles. Part (c) shows a novel construction of the 3D associahedron K_5, with 7 elements partitioned into 4 bundles. Figures 11 and 12 provide detailed truncation constructions of (b), whereas Figures 9 and 10 do so for (c).

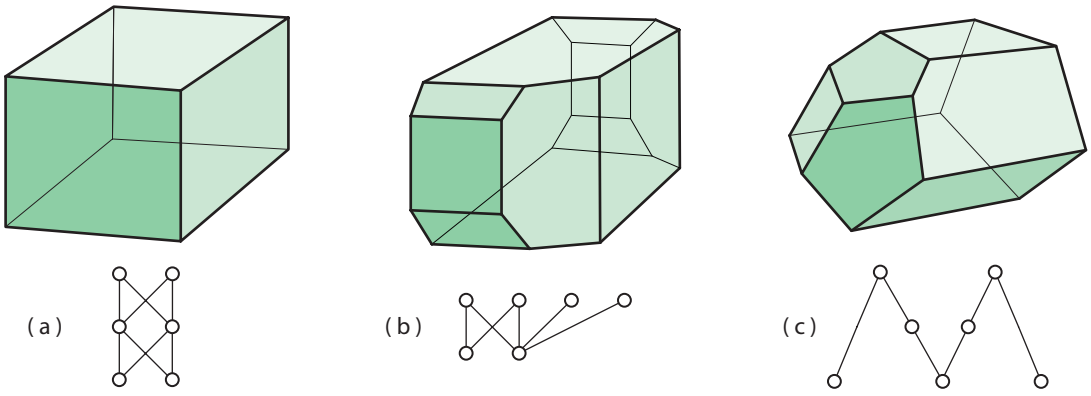

FIGURE 5. Examples of 3D poset associahedra.

2.3. The notion of being "filled" appears in different guises: For a graph associahedron $\mathcal{K}G$ and its underlying simple graph G, a *tube* of G is filled because it is an induced subgraph, catalogued just by listing the vertices of G [3, Section 2]. A graph *tubing* is filled because its tubes are "far apart," which is equivalently described by saying that two distinct tubes in a tubing cannot have a single edge connecting them. Since a non-minimal bundle of a simple graph must be a singleton bundle, the following is immediate:

Proposition 5. *The graph associahedron $\mathcal{K}G$ can be obtained as a poset associahedron $\mathcal{K}P$, where P is the face poset of graph G.*

For pseudographs (having loops and multiple edges), a filled tube is a connected subgraph t where at least one edge between every pair of nodes of t is included if such edges exist [4, Section 2]. For multiple edges of G, the notion of tubes on posets match perfectly with tubes on G, and the proposition above extends to the pseudograph associahedron. The first three examples of Figure 6 displays invalid tubings (all due to not being filled) and the last a valid one; the top row shows tubes on graphs whereas the bottom recasts them on posets.

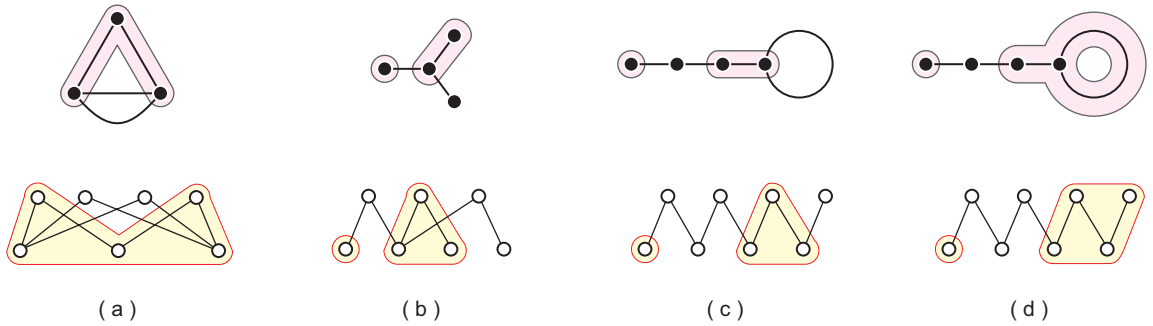

FIGURE 6. Graphs and posets, where (a), (b), (c) are invalid tubings, whereas (d) is a valid tubing.

Remark. For each loop attached to a node v of G, the pseudograph associahedron defined in [4] gave a choice of choosing or ignoring the loop when v is chosen in a tube; see Figure 6(c) and (d). In this paper, however, for the sake of consistency in the notion of "filled", we always include at least one loop for poset associahedron. This allows us to always obtain convex polytopes, rather than unbounded polyhedral chambers of [4].

The notion of *associativity*, encapsulated by drawing tubes on graphs, has a natural generalization to higher-dimensional complexes. In particular, for any CW-complex structure X, consider its face poset P_X. The poset associahedron $\mathcal{K}P_X$ captures the analogous information of X that the graph associahedron captures for a graph.

Example. Figure 7(a) shows a CW-complex, with three 2-cells, 1-cells, and 0-cells. Part (b) shows the poset structure of this complex, and (c) its poset associahedron.

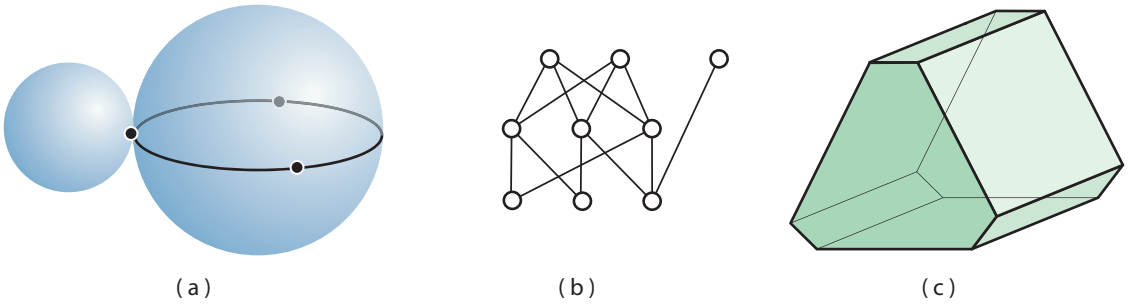

FIGURE 7. The poset associahedron of a CW-complex.

3. CONSTRUCTIONS

3.1. The poset associahedron $\mathcal{K}P$ is recursively built by a series of truncations, as described by the following theorem. This immediately implies the combinatorial result of Theorem 2.

Theorem 6. *Let P be a connected poset. The poset associahedron $\mathcal{K}P$ is constructed inductively on the number of elements of P. Choose a maximal element x of a maximal length chain of P.*

(1) *If bundle $\mathfrak{b}_x$ is singleton, truncate certain faces of $\mathcal{K}(P-x)$ to obtain $\mathcal{K}P$.*
(2) *If bundle $\mathfrak{b}_x$ is non-singleton, truncate certain faces of $\mathcal{K}\left(P-(\mathfrak{b}_x-x)\right)\times\Delta_{|\mathfrak{b}_x-x|}$ to obtain $\mathcal{K}P$.*

Because this truncation procedure is delicate, we present an overview and details here, and save the remainder of the proof for Section 5. For the rest of this section, let x be a maximum element in a maximal chain of P.

Consider the first case in Theorem 6, where bundle $\mathfrak{b}_x$ is a singleton. Note that a tube t of P either contains x or not. If not, then t must be a tube of $P-x$, a filled connected lower set in $P-x$, and not containing ∂x. If t does contain x, then $t-x$ is unfilled, resulting in (possibly several) disconnected tubes, each containing some of ∂x. The following definition goes in reverse, "filling up" a pairwise disjoint tubing of $P-x$.

Definition. For a singleton bundle $\mathfrak{b}_x$, and for a pairwise disjoint tubing T of $P-x$, let

$$\mathrm{fill}_x(T) \;:=\; \{x\} \;\cup\; \{p\in t \mid t\in T\}\,.$$

Figure 8 gives some examples.

We construct the new polytope $\mathcal{K}P$ by truncating certain faces of $\mathcal{K}(P-x)$. Begin by marking any face T of $\mathcal{K}(P-x)$ in which $\mathrm{fill}_x(T)$ becomes a tube of P. Truncate these marked faces iteratively, ordered in *decreasing* size of the $\mathrm{fill}_x(T)$ tubes; the order of truncation is arbitrary for ties. The original facets of $\mathcal{K}(P-x)$ retain their tube labeling in $\mathcal{K}P$, whereas

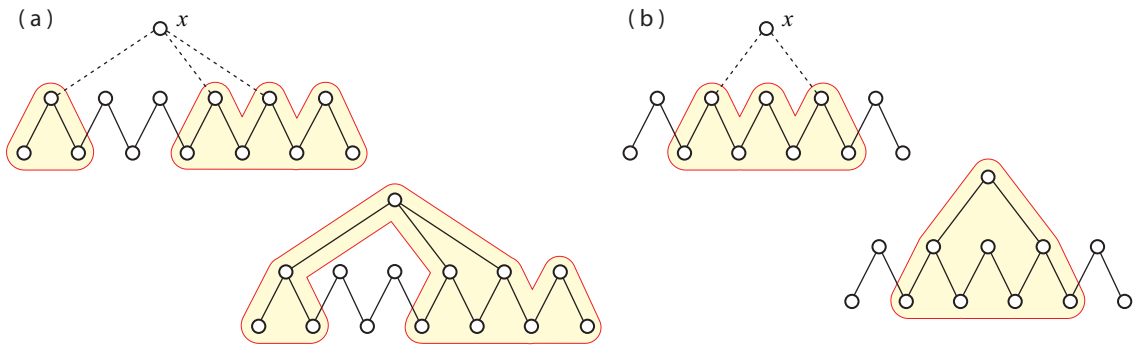

FIGURE 8. Tubing T of $P - x$ (top row) and $\text{fill}_x(T)$ of P (bottom row).

the new facets formed from truncation inherit their associated $\text{fill}_x(T)$ tube labels. As always, each face of $\mathcal{K}(P)$ is labeled with a tubing, the set of tubes of its incident facets.

Example. Figure 9 shows the polytope $\mathcal{K}(P-x)$, a pentagonal prism, along with the labeling of its facets. The pentagon appears in Figure 4(a), and the addition of the disconnected element of the poset yields, by Proposition 3, a product with Δ_1. In order to construct $\mathcal{K}P$, by including the maximal element x, we first notice that $\mathfrak{b}_x$ is singleton. Two edges of the

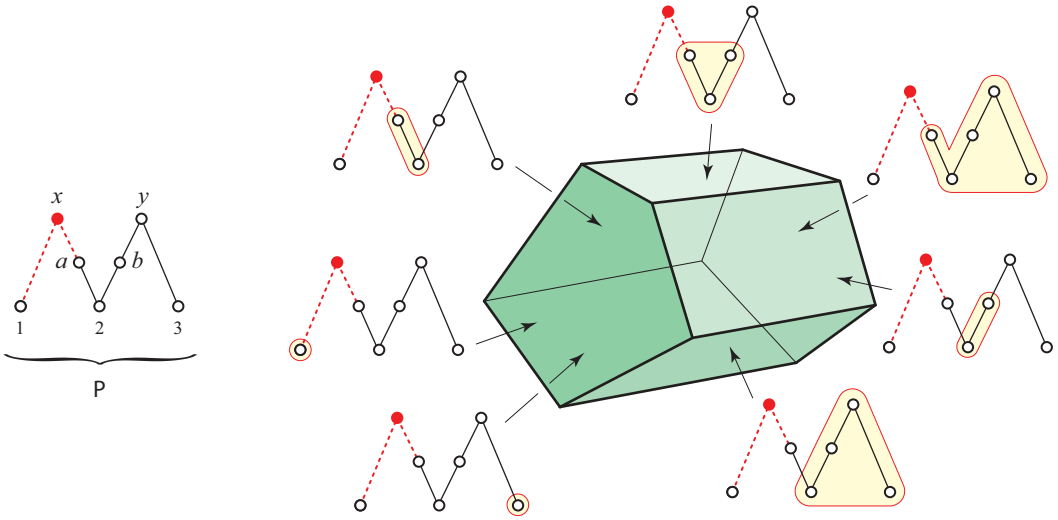

FIGURE 9. The labeling of the facets of $\mathcal{K}(P - x)$, a pentagonal prism.

prism need to be truncated, as labeled on the left side of Figure 10; these are the unique faces T of $\mathcal{K}(P - x)$ where $\text{fill}_x(T)$ are tubes of P. One edge has five elements in $\text{fill}_x(T)$, and the other has four, and they are truncated in decreasing size of their tubes. The resulting $\mathcal{K}P$ is displayed on the right side, along with the updated labeling of the two new facets.

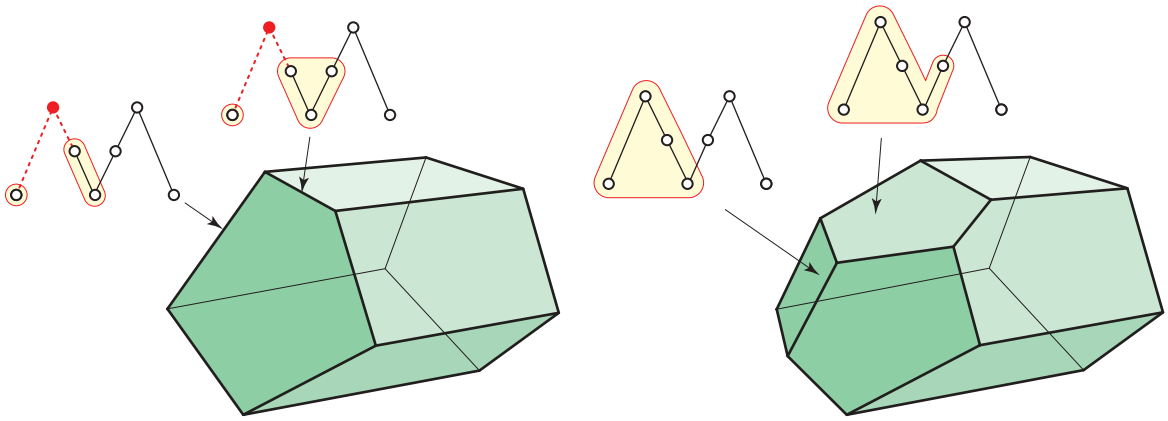

FIGURE 10. Truncating edges in decreasing order of tube size, resulting in $\mathcal{K}P$.

3.2. As before, let x be a maximum element in a maximal chain of P, and consider the second case in Theorem 6, when bundle $\mathfrak{b}_x$ is non-singleton. Construct the new polytope $\mathcal{K}P$ by truncating certain faces of

$$\mathcal{K}P_* \;:=\; \mathcal{K}(P-(\mathfrak{b}_x-x)) \;\times\; \Delta_{|\mathfrak{b}_x-x|}\,,$$

where the vertices of $\Delta_{|\mathfrak{b}_x-x|}$ are labeled with the elements of $\mathfrak{b}_x$, and its faces by the subset of vertex labels they contain. Thus, faces of $\mathcal{K}P_*$ get labeled by the pairing (T, B), for the corresponding tubing[1] T of $\mathcal{K}(P-(\mathfrak{b}_x-x))$ and subset B of $\mathfrak{b}_x$.

Remark. Consider the poset $P-(\mathfrak{b}_x-x)$, along with $|\mathfrak{b}_x-x|$ isolated elements. Proposition 3 outlines a polytope associated to this disconnected poset. Although $\mathcal{K}P_*$ is isomorphic to this polytope, the labeling of their faces are fundamentally different.

Example. Figure 11 shows the polytope $\mathcal{K}P_*$, a combinatorial cube, where bundle $\mathfrak{b}_x = \{x, y\}$ is non-singleton. This cube is the product of the square from Figure 4(b), and the simplex Δ_1 whose vertices are labeled by $\mathfrak{b}_x$. The six facets of $\mathcal{K}P_*$ are appropriately labeled by tubes, along with their associated subset $B \subset \mathfrak{b}_x$ below each tube.

In order to obtain the new polytope $\mathcal{K}P$ from truncations of $\mathcal{K}P_*$, begin by marking any face (T, B) of $\mathcal{K}P_*$ where the tubing $T = \{t\}$, for some tube $t \ni x$. Truncate these marked faces iteratively, ordered in *increasing* size of the $\{t-x\} \cup B$ tubes; the order of truncation is arbitrary for ties. These new facets inherit the $\{t-x\} \cup B$ tube label in $\mathcal{K}P$, and any untruncated facets (T, B) of $\mathcal{K}P_*$ simply retain their T label, discarding the B coordinate. As always, each face of $\mathcal{K}(P)$ is labeled with a tubing, the union of tubes of its incident facets.

[1]Here, we allow the tubing T that contains the single "universal" tube $P-(\mathfrak{b}_x-x)$, which labels the interior of the polytope $\mathcal{K}(P-(\mathfrak{b}_x-x))$.

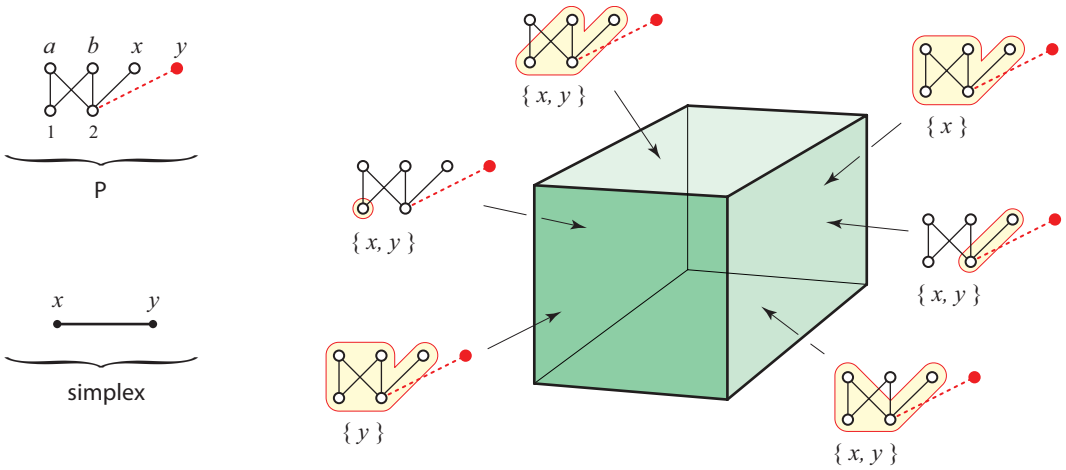

FIGURE 11. The labeling of the facets of the cube $\mathcal{K}P_*$.

Example. Continuing the case from Figure 11, six edges of $\mathcal{K}P_*$ must be truncated to obtain $\mathcal{K}P$. Figure 12(a) shows the first two edges to be truncated, followed by the remaining four in (b), resulting in $\mathcal{K}P$ as seen in (c).

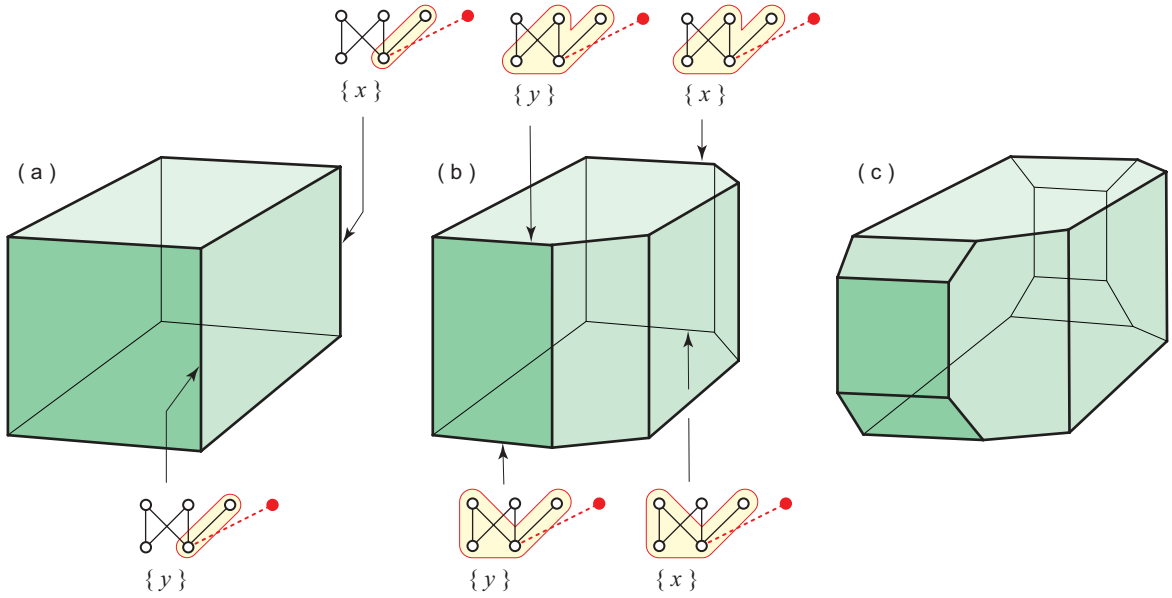

FIGURE 12. Truncating six edges in increasing order of tube size, resulting in $\mathcal{K}P$.

Figure 13 shows the $\mathcal{K}P_*$ labels of these six truncated edges on the top row, along with their updated $\{t - x\} \cup B$ tube labels in $\mathcal{K}P$ immediately beneath each one. Five of the six facets of $\mathcal{K}P_*$ also need to be truncated, as given by the bottom rows of Figure 13. Although truncating facets does not alter the combinatorics of the polytope, it causes their facet labels to be updated by the algorithm. The sixth facet of $\mathcal{K}P_*$, shown in the bottom right, is not

truncated but relabeled by simply forgetting its B label. The combinatorics of this facet, appearing as an octagon in $\mathcal{K}P$, are analyzed further in Figure 19.

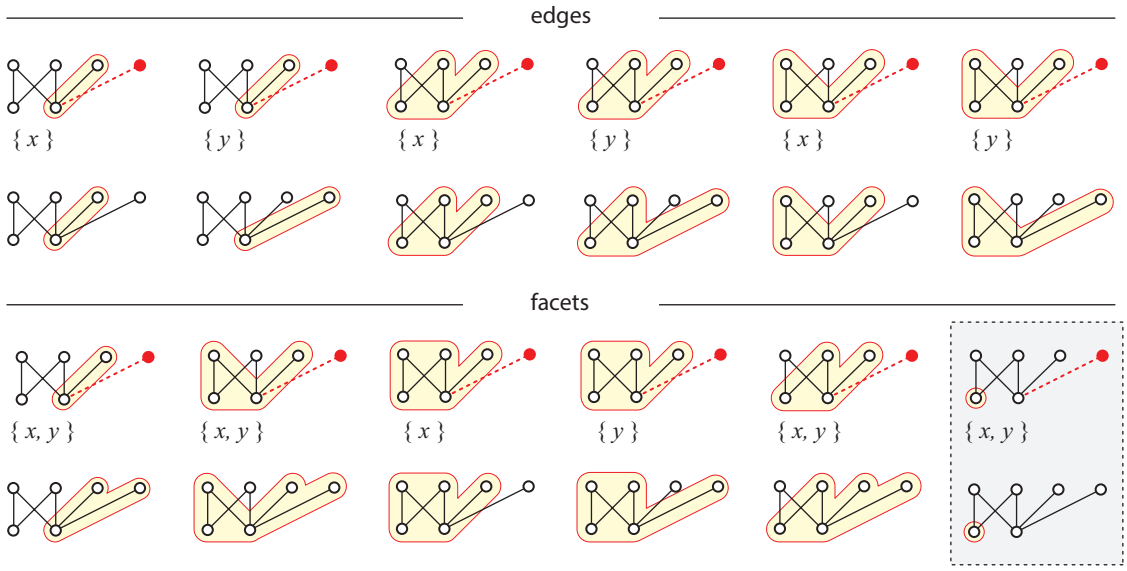

FIGURE 13. Labels of the edges and facets of $\mathcal{K}P_*$ that are truncated (rows 1 and 3), along with their updated labels in $\mathcal{K}P$ (rows 2 and 4). The sixth facet, shown in the bottom right, is not truncated but relabeled.

Example. A 4D case for Theorem 6 is provided in Schlegel diagram on the right side of Figure 14, where the poset steps are drawn above. Part (a) begins with the poset P_o of Figure 5(b). In Figure 14(b), by Proposition 4, adding the new maximal element to this poset does not change the structure of the polytope. Finally, part (c) shows the addition of a non-singleton bundle, now with two elements. According to Theorem 6, we first consider the 4D polytope $\mathcal{K}P_* = \mathcal{K}P_o \times \Delta_1$, the left Schlegel diagram of Figure 14. Then truncate certain faces (first the two blue chambers, then the four orange ones) to obtain the 4D poset associahedron drawn on the right. Note that these truncations mimic the construction in Figure 12 for one dimension higher.

3.3. The following is a notable consequence of Theorem 6:

Proposition 7. *There are different ways to construct $\mathcal{K}P$, based on the possible choices of maximal elements in the recursive process.*

We close this section with a corollary of this proposition as it pertains to the classical associahedron K_n. Interestingly, this construction of the associahedron is novel, though examples of special cases have appeared in different parts of literature, as referenced below.

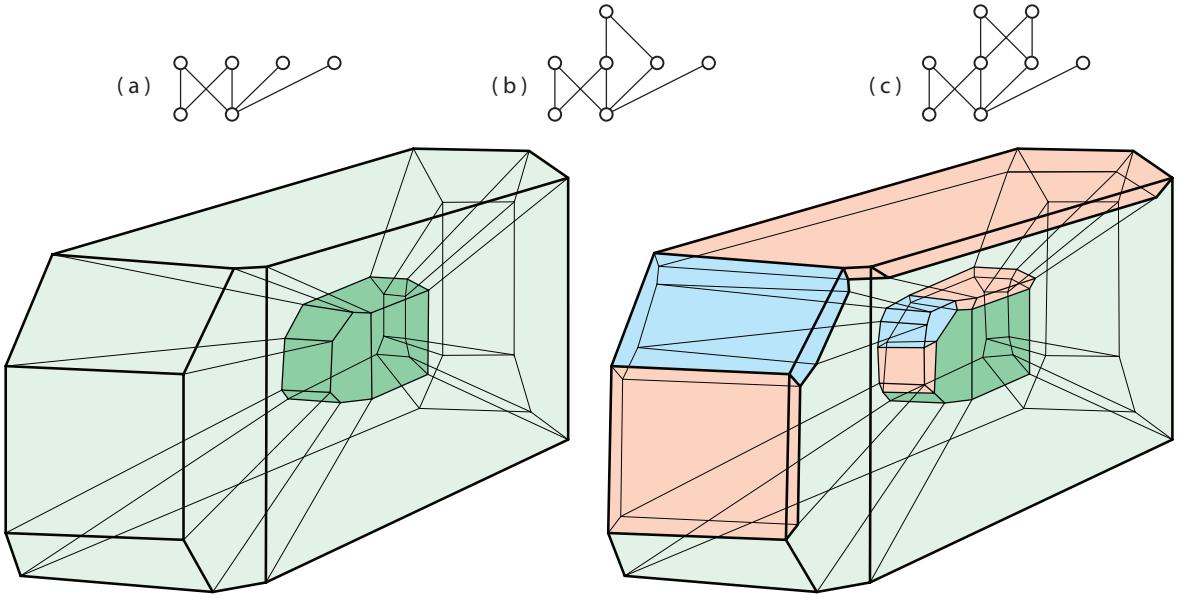

FIGURE 14. Construction of a 4D poset associahedron.

Proposition 8. *The poset associahedron of the* zigzag *poset with* $2n-1$ *elements yields the classic associahedron* K_{n+1}*. In particular, the associahedron* K_{n+1} *is obtained by truncations of codimension two faces of* $K_{p+1} \times \Delta_1 \times K_{q+1}$*, where* $n = p + q$ *and* $p, q \geq 1$*.*

Proof. The poset P of a path G with n nodes is the zigzag poset with $2n-1$ elements; the tubings on P resulting in $\mathcal{K}P$ are in bijection with tubes on the graph G. The enumeration of the different types of truncation comes from removing a maximal element of P and using Theorem 6(b). □

Remark. The particular construction of K_{n+1} from $K_n \times \Delta_1 \times K_2 \simeq K_n \times \Delta_1$ appears in another form in the work by Saneblidze and Umble [15] on diagonals of associahedra.

Example. Figure 15 considers one construction of the 3D associahedron: Part (a) begins with the pentagon from Figure 3(a), and (b) adds an extra disconnected element. By Proposition 3, the result is the product with Δ_1, a pentagonal prism. Part (c) connects up the poset with a singleton bundle; two edges of the prism are truncated according to the proof of Theorem 6 to yield the associahedron. Indeed, Figure 5(c) is formed in an identical manner.

Example. Figure 16 considers another assembly of the 3D associahedron: Each disconnected component yields an interval, and together (by Proposition 3), the result is a cube (a), the product of three intervals $K_3 \times \Delta_1 \times K_3$. Part (b) connects up the poset with a singleton bundle, and three of its edges are truncated according to the proof of Theorem 6. This

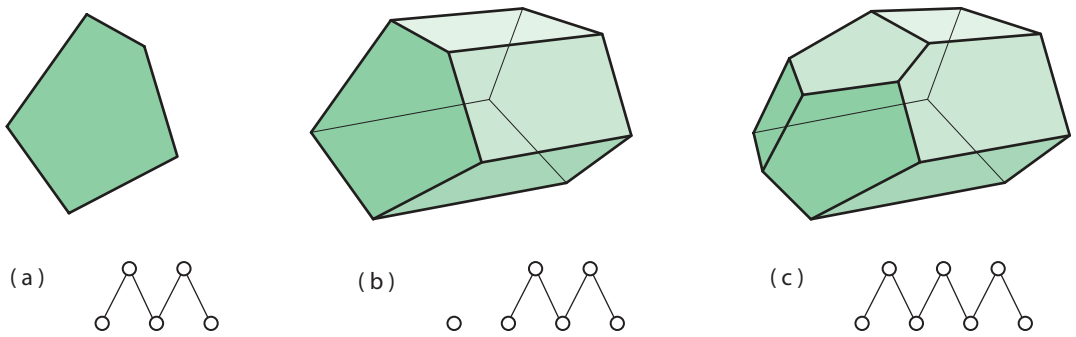

FIGURE 15. The associahedron K_5 from a pentagonal prism, $K_4 \times \Delta_1 \times K_2$.

construction appears in the work of Buchstaber and Volodin [2], motivated by truncating codimension two faces of cubes.

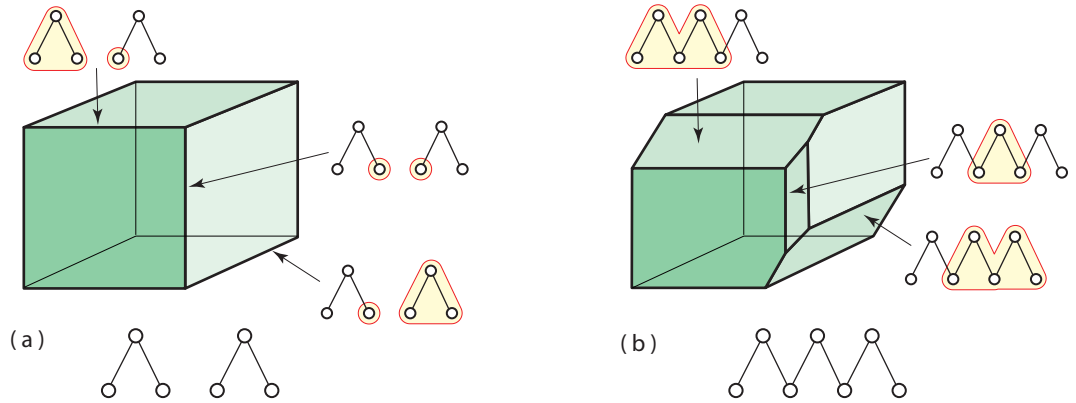

FIGURE 16. The associahedron K_5 from a cube, $K_3 \times \Delta_1 \times K_3$.

Example. In a similar vein, Figure 17 obtains the 4D associahedron K_6 (right side) from truncating five codimension two faces of $K_4 \times \Delta_1 \times K_3$ (left side). The order of truncation is important: first the two blue faces, then two orange faces, and finally one yellow face.

4. Family of Associahedra

4.1. The $(n-1)$-dimensional permutohedron $\mathcal{P}_n$ is the convex hull of the points formed by the action of a finite reflection group on an arbitrary point in Euclidean space. The classic example is the convex hull of all permutations of the coordinates of the Euclidean point $(1, 2, \ldots, n)$. Changing edge lengths while preserving their directions results in the *generalized permutohedron*, as defined by Postnikov [14]. An important subclass of these is the *nestohedron*, a polytope based on the combinatorics of a building set [18].

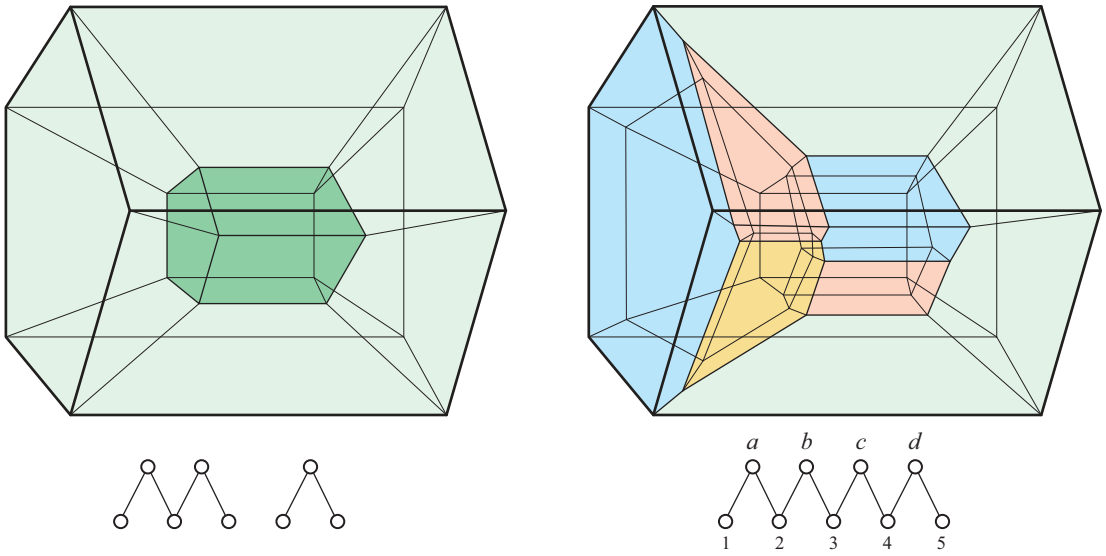

FIGURE 17. The associahedron K_6 from $K_4 \times \Delta_1 \times K_3$.

Recall that a building set in a finite Boolean lattice is a collection $\mathcal{B}$ of nonempty subsets of a ground set S. The building set must contain all singletons $\{s\}$, for $s \in S$, and for any two elements of the building set that intersect, their union must also be an element of $\mathcal{B}$. This latter requirement has a nice geometrical interpretation: it guarantees that the nested set polytope of the building set, the nestohedron $N(\mathcal{B})$, can be created by truncating the faces of the simplex that correspond to the elements of the building set. Our invention is a generalization of building set that weakens the intersection/union property for elements, making it so that this set need not live in a lattice. We have the following condition instead:

Lemma 9. *If t_1 and t_2 are tubes of poset P that intersect, then there exists a tube t_* (possibly all of P) containing their union.*

Proof. Since unions of lower sets are lower sets, and since t_1 and t_2 intersect, their union must be a connected lower set. If $t_1 \cup t_2$ is not a tube, construct t_* by adding an element of P from each bundle whose boundary is in the union. If the result is not a tube (due to newly included boundaries), iterate this process until no additions are necessary. □

The next two results establish a strong relationship between nestohedra and poset associahedra, with posets of rank two.

Theorem 10. *Any nestohedron is combinatorially equivalent to a poset associahedron $\mathcal{K}P$, for some poset P of rank two, whose non-minimal bundles are all singletons.*

Proof. Given a building set $\mathcal{B}$ of a set S, we describe a rank two poset $P_{\mathcal{B}}$, whose tubes are in bijection with $\mathcal{B}$ and whose tubings are in bijection with the nested sets of $\mathcal{B}$. The poset $P_{\mathcal{B}}$

has minimal elements given by set S, and has maximal elements (each a singleton bundle) given by set $\mathcal{B}$, each having boundary exactly the minimal elements that it contains.

The tubes of $P_{\mathcal{B}}$ are the lower sets of $P_{\mathcal{B}}$ that are generated by certain sets X, made up of height two elements of $P_{\mathcal{B}}$: To create such a set X, choose a height two element $A \in \mathcal{B}$ and then include with it all other height two elements contained in A. The lower set generated by this set is automatically filled and connected, and all tubes are achieved in this way. Thus, each tube corresponds to an element of $\mathcal{B}$ by taking the set of minimal elements of $P_{\mathcal{B}}$ that lie in the tube.

The rules that define a tubing T of $P_{\mathcal{B}}$ also define a nested set of the building set $\mathcal{B}$, via the same correspondence: Pairs of tubes in T must be either disjoint or nested, and this property is mirrored by their respective sets of minimal elements. Moreover, a subset Y of tubes has a union that is not filled if and only if the set of minimal elements of that union Y is precisely the boundary of a height two element (which is not itself in Y, by construction of $P_{\mathcal{B}}$). The ordering of nested sets by reverse inclusion corresponds to the ordering of tubings by reverse inclusion, so the nestohedron $N(\mathcal{B})$ is isomorphic to our polytope $\mathcal{K}P_{\mathcal{B}}$. □

Example. Note that $P_{\mathcal{B}}$ is one of many posets whose polytope is $N(\mathcal{B})$; many more rank two posets can often be found: Given set $S = \{1, 2, 3, 4\}$ and building set

$$\mathcal{B} \;=\; \{\{1\}, \{2\}, \{3\}, \{4\}, \{12\}, \{23\}, \{123\}, \{124\}, S\}\,, \tag{4.1}$$

Figure 18(a) shows the poset $P_{\mathcal{B}}$ constructed in the proof of Theorem 10. Moreover, all the posets in this figure result in combinatorially equivalent poset associahedra.

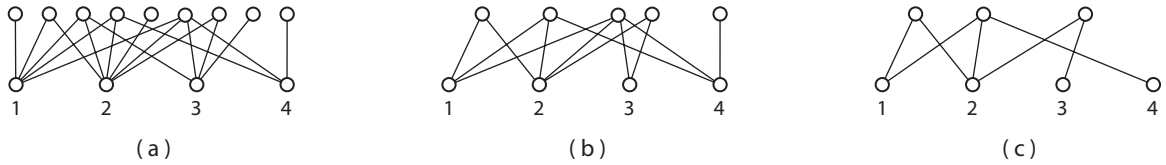

FIGURE 18. Examples of different posets resulting in identical poset associahedra.

Theorem 11. *For any poset P whose non-minimal bundles are all singletons, the poset associahedron $\mathcal{K}P$ is combinatorially equivalent to a nestohedron.*

Proof. Let S be the set of minimal elements of poset P. Consider the set $\mathcal{B}(P)$ of subsets of S whose elements are the sets of minimal elements of tubes. It is not difficult to realize that $\mathcal{B}(P)$ is a building set, following Lemma 9. Notice that finding $\mathcal{B}(P)$ for the posets in Figures 18(b) and (c) yield the same building set $\mathcal{B}$ given in (4.1) above. We claim there is an isomorphism of posets between the tubings of P and the nested sets of $\mathcal{B}(P)$, where each tube of a tubing T is mapped to the set of its minimal elements. This mapping is an injection

because each tube is uniquely determined by its set of minimal elements (since P has only singleton non-minimal bundles).

We claim that the image of this mapping is a nested set for $\mathcal{B}(P)$. Given that every pair of tubes in T is nested or disjoint, the same is implied for their respective sets of minimal elements. Note that a collection of disjoint sets of minimal elements of disjoint tubes has a union that is the minimal set of a tubing that is filled. It then follows that the union of those sets of minimal elements is not in $\mathcal{B}(P)$, since the span of that union is not a tube. Finally, the map preserves ordering by inclusion, since one collection of sets of minimal elements is included in another if and only if the tubes they span are a subset of the tubes spanned by the other. □

4.2. Although poset associahedra contain nestohedra, they are a different class than generalized permutohedra. For instance, Figure 5(b), detailed in Figure 12(c), shows a 3D polytope which has an octagonal face, something not possible for generalized permutohedra. Figure 19 below shows this octagon in detail. Similarly, the 4D example in Figure 14 is not a nestohedron as well.

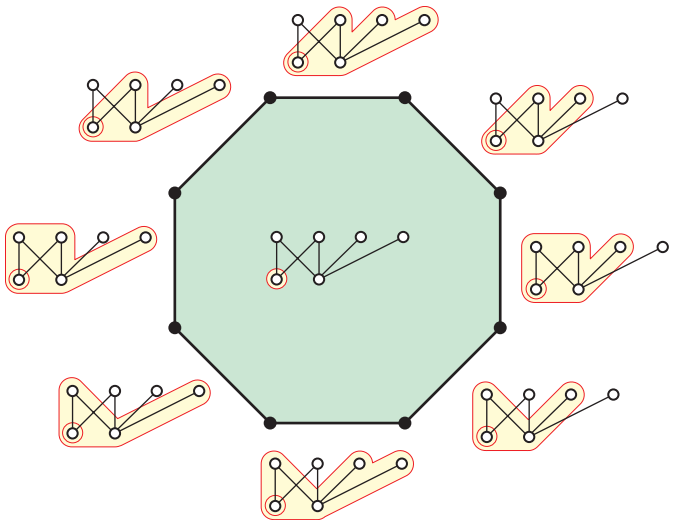

FIGURE 19. Octagonal face of the polyhedron in Figure 5(b).

All graph associahedra and nestohedra are obtained from rank two posets, and it is natural to ask whether all poset associahedra can be obtained from some rank two posets. For instance, the rank three poset of Figure 4(a) yields the same $\mathcal{K}P$ as the rank two poset of Figure 3(a). The following shows that higher ranks indeed hold deeper structure.

Proposition 12. *There exists poset associahedra $\mathcal{K}P$ which cannot be found as $\mathcal{K}P'$, for any poset P' of rank two.*

Proof. Consider the 4D example in Figure 14, a rank three poset associahedron with f-vector $(68, 136, 88, 20)$. Since this is not a nestohedron, Theorem 11 shows that at least one non-singleton bundle is needed when restricting to rank two. Using computer calculations [19], we enumerated the f-vectors of all 4D poset associahedra for rank two posets and at least one non-singleton bundle. For each polytope with a matching f-vector (for around 500 posets), we verified using the *Sage* software [17] that it was not equivalent to the one in Figure 14. □

Remark. There is also a simple connection between posets and hypergraphs: Start with set S and create any number of new maximal elements, each of which covers some of S, where each maximal element is a singleton bundle. The set of tubes of such a poset P will yield a building set $\mathcal{B}$ on the set of minimal elements of P, due to the definition of a tube as a connected filled lower set. This amounts to choosing a subset of the power set of S (a *hypergraph* on S), and thus the process of building $\mathcal{K}P$ for such a poset is akin to constructing the hypergraph polytope [9].

4.3. We close with some examples relating $\mathcal{K}P$ to the classical permutohedron $\mathcal{P}_n$.

Proposition 13. *Let $\mathfrak{b}_x$ be a bundle with n elements of a poset P such that all of its elements are maximal. If $\partial x = P - \mathfrak{b}_x$, then $\mathcal{K}P = \mathcal{K}(P - \mathfrak{b}_x) \times \mathcal{P}_n$.*

Proof. A tubing $U \in \mathcal{K}P$ containing no tubes that intersect $\mathfrak{b}_x$ can be viewed as a tubing in $\mathcal{K}(P - \mathfrak{b}_x)$; call it $\alpha(U)$. Let $V \in \mathcal{K}P$ be a tubing with only tubes that intersect $\mathfrak{b}_x$, where a tube in V is a lower set generated by a subset of $\mathfrak{b}_x$, and compatibility of these tubes is equivalent to the subsets being nested.

Label the nodes of the complete graph Γ_n with the elements of the bundle $\mathfrak{b}_x$. Let $\beta(V)$ be the tubing on Γ_n such that if $t \subset \mathfrak{b}_x$ generates a tube in V, t is a tube in $\beta(V)$. Any tubing $T \in \mathcal{K}P$ can be written as a tubing U and a tubing V, where the map $T \to (\alpha(U), \beta(V))$ preserves compatibility and is bijective. The proof follows since the graph associahedron of a complete graph of n nodes is the permutohedron $\mathcal{P}_n$. □

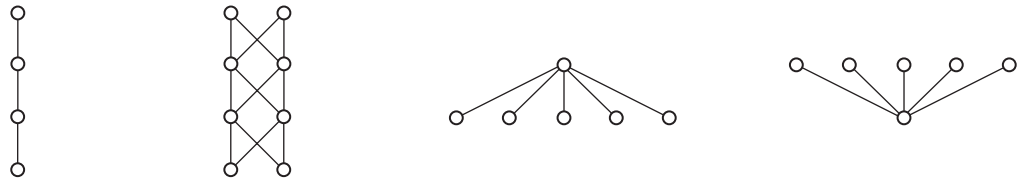

(a) *point* (b) *cube* (c) *simplex* (d) *permutohedron*

FIGURE 20. Examples of simple posets.

Corollary 14. *Consider Figure 20. If (a) P is a chain, (b) a cross-stack of rank n, (c) a rank one element with $n+1$ boundary elements, or (d) a bundle with one minimal and n maximal elements, then $\mathcal{K}P$ is a point, an n-cube, an n-simplex, or $\mathcal{P}_n$, respectively.*

Proof. This follows from Propositions 3, 4, and 13. □

5. Proofs

5.1. The proof of Theorem 6 is now given, which immediately results in Theorem 2. We proceed by (strong) induction on the size of the poset P, creating a poset isomorphism between the face poset of the newly constructed $\mathcal{K}P$ and tubings of P. We often speak of and illustrate this isomorphism as a labeling of the polytope faces with tubings. The reader is encouraged to recall the notations and definitions found in Section 3.

The base case of our induction is the trivial case of a singleton poset. If P is disconnected, we know by induction that each connected part P_i is isomorphic to the face poset of $\mathcal{K}P_i$. Thus $\pi(P)$ is isomorphic to $\mathcal{K}P$ defined as the cartesian product in Proposition 3. If P is connected, then for the inductive step we begin by choosing an element $x \in P$ that is the maximum element in a maximal chain of P. There are two cases, depending on whether x is the only element in its bundle or not.

Proposition 15. *For a singleton bundle $\mathfrak{b}_x$, there exists a poset isomorphism f from the poset of tubings $\pi(P)$ to the simple polytope $\mathcal{K}P$, found by truncating $\mathcal{K}(P-x)$, as described in Section 3.*

Proof. By induction, there is poset isomorphism g from the face poset of the simple polytope $\mathcal{K}(P-x)$ to the poset of tubings $\pi(P-x)$. The facets of the truncated polytope $\mathcal{K}P$ are clearly in bijection with the tubes of P: the tubes of P either do not contain x (and so are present by induction), or do contain x (and are introduced by truncation). We show that f is an isomorphism of posets from $\pi(P)$ to $\mathcal{K}P$ by checking that facets $f(t)$ of $\mathcal{K}P$ intersect in a face $f(T)$ if and only if their respective tube labelings t form a tubing T of P. Since we are dealing with convex polytopes (where every set of facets intersects in a unique face, if at all), this simultaneously shows that f is a bijection of tubings and preserves the ordering of tubings.

Forward direction: Let T be a set of tubes that is not a tubing of poset P. We show the set of facets $\{f(t) \mid t \in T\}$ has empty intersection. Since P is connected, there is either

(1) a pairwise disjoint subset $S \subset T$ whose union is unfilled in P, or
(2) there is a pair of nonnested but intersecting tubes in T.

First consider the former case, when the union of S is unfilled. Adding x to this union will make it either a filled lower set or not. If the union of $\{x\}$ and the tubes in S is filled, then our

truncations will have effectively separated the facets $f(t)$ labeled by tubes $t \in S$ by removing their intersection.[2] On the other hand, if adding x to the union of S does not make a filled set, then, because our inductive assumption about $\mathcal{K}(P-x)$ guarantees that $\{g(t) \mid t \in S\}$ is empty, $\{f(t) \mid t \in S\}$ will be empty as well.

Now consider the latter case, when T contains intersecting, nonnested tubes, say t_1 and t_2 of P. The facets $f(t_1)$ and $f(t_2)$ have empty intersection when neither tube contains x, due to our inductive assumption on $\mathcal{K}(P-x)$. So let one or both tubes contain x. Lemma 9 claims there must exist a unique smallest tube of t_* of P containing their union.

Without loss of generality, we assume $x \in t_1$ and let T_1 be the disjoint tubing of $P-x$ such that $t_1 = \mathrm{fill}_x(T_1)$. If $x \in t_2$, let $t_2 = \mathrm{fill}_x(T_2)$; else, let $T_2 = \{t_2\}$. Note that only the case where $T_1 \cup T_2$ is a tubing of $P-x$ need be considered, for otherwise, induction claims the two faces $g(T_1)$ and $g(T_2)$ did not intersect in $\mathcal{K}(P-x)$. Since $T_1 \cup T_2$ is a tubing and does not cover $P-x$, then $t_* \neq P$, implying $f(t_*)$ was formed by truncation. Thus, $t_* = \mathrm{fill}_x(T_*)$, for a tubing T_* of disjoint tubes, each containing some of ∂x. Because t_* is larger than either t_1 or t_2, the truncation of $g(T_*)$ will occur before either truncation of $g(T_1)$ or $g(T_2)$.

In order to conclude that $f(t_1)$ and $f(t_2)$ (associated to the truncations of $g(T_1)$ and $g(T_2)$) will not intersect in $\mathcal{K}P$, we need to show that

$$g(T_1) \,\cap\, g(T_2) \;=\; g(T_1 \cup T_2) \;\subset\; g(T_*)\,,$$

which follows if $T_* \subset T_1 \cup T_2$. To show this, consider the partition $\{u_1, \ldots, u_k\}$ of ∂x into its set of disjoint connected lower sets. Since $T_1 \cup T_2$ is a tubing of $P-x$, the smallest tube $t_* = \mathrm{fill}_x(T_*)$ containing all the tubes in T_1 and T_2 contains no elements of P outside those tubes except for x. Therefore, T_* is the set of tubes appearing in the list $\{t_1, \ldots, t_k\}$, where t_i is the largest tube in $T_1 \cup T_2$ with $u_i \subset t_i$. Thus, the tubes of T_* must be as described, and the conditions needed are fulfilled.

Example. For an instance of just one tube containing x, consider Figures 9 and 10. If $t_1 = \{1, 2, a, x\}$ and $t_2 = \{2, a, b\}$, then $T_1 = \{\{1\}, \{2, a\}\}$ and $T_2 = \{\{2, a, b\}\}$. Therefore, $T_* = \{\{1\}, \{2, a, b\}\}$ and the face it labels is truncated first, and given by $t_* = \{1, 2, a, b, x\}$. For an example of both tubes containing x, consider Figure 17. The facets in question are the two orange ones in the associahedron: they are labeled by the tubes $\{2, 3, 4, b, c\}$ and {3,4,5,c,d}. They do not intersect by virtue of the blue facet between them, labeled by $\{2, 3, 4, 5, b, c, d\}$. The latter was created by truncation previous to either orange facet. Note also that this shows that the orange facets can be formed by truncation in either order.

[2]This is because that intersection must have been contained in a truncated face. For instance, consider the poset P in Figures 9. Due to truncation, the facets labeled by $S = \{\{1\}, \{2, a\}, \{3\}\}$ intersect in Figure 9 but not in Figure 10.

Backward direction: Let $t_1, \ldots, t_m$ be the new tubes of P, those tubes which contain x and whose facets $f(t_i)$ are formed by truncation. Using finite induction on m, we show that if T is a tubing of P, then $\{f(t) \mid t \in T\}$ has nonempty intersection. Let S_i be the set of disjoint tubes of $P - x$ such that $t_i = \text{fill}_x(S_i)$. Associated to T is a tubing T_0 of $P - x$ made of the following tubes:

(1) The tubes $t \not\ni x$ of T,
(2) For each tube $t_i \ni x$ of T, the set S_i of disjoint tubes of $P - x$.

Our argument considers the series of all truncations that are performed on $\mathcal{K}(P - x)$: as truncations are performed, the set T_0 is updated, evolving to become the tubing T. At each intermediate stage, we claim that the set of tubes labels a set of facets that has nonempty intersection. Recursively define the intermediate set of tubes T_k, whose truncations create facets $f(t_1), \ldots, f(t_k)$, as follows:

$$T_k \;:=\; (T_{k-1} - S_k) \;\cup\; (S_k \;\cap\; (T \;\cup\; \mathfrak{S}_k)) \;\cup\; (\{t_k\} \cap T)\,,$$

where $\mathfrak{S}_k = \bigcup \{S_i \mid i > k,\ t_i \in T\}$. Indeed, after all m truncations, we will have transformed T_0 to become $T_m = T$, by adding to the list of tubes in T_0 all the new tubes $t_i = \text{fill}_x(S_i)$ in T, and subtracting all the tubes of T_0 which are not in T.

Example. Consider the tubing $T = \{\{1\}, \{1,2,a,x\}, \{1,2,a,b,x\}\}$ from Figures 9 and 10. Here, $T_0 = \{\{1\}, \{2,a\}, \{2,a,b\}\}$, $T_1 = \{\{1\}, \{2,a\}, \{1,2,a,b,x\}\}$, and $T_2 = T$.

We now establish our claim. The base case follows from the induction hypothesis (on the number of elements in our poset) that facets labeled by the tubes of T_0 do intersect at a unique face of the simple polytope $\mathcal{K}(P - x)$. Next, assume that after truncating to create facets $f(t_1), \ldots, f(t_{k-1})$, the facets labeled by the tubes in T_{k-1} do indeed intersect. We use this assumption to show that truncating to create the facet $t_k = \text{fill}_x(S_k)$ will preserve the property of nonempty intersection once more, for T_k.

First, consider the case where tube $t_k \ni x$ is not in T. Notice then that $T_k = T_{k-1}$. Since $t_k = \text{fill}_x(S_k)$ is not in T, then S_k is not contained by T_{k-1}, and therefore, the face labeled by S_k does not contain the intersection of facets labeled by tubes of T_k. Thus, the truncation does not separate the facets labeled by the tubes in T_k.

Now consider the case where $t_k \in T$. First we check that the facets labeled by

$$T_k \;\cap\; T_{k-1} \;=\; T_k \;-\; \{t_k\} \tag{5.1}$$

have a nonempty intersection, after truncating the face labeled by S_k. This will be true if S_k is not contained by $T_k - \{t_k\}$. We show that at least one tube in S_k will be removed from the list when we update T_{k-1} to T_k: that is, in view of our algorithm, we show that not all the tubes of S_k are found in the union $T \cup \mathfrak{S}_k$.

Since truncation occurs in decreasing order of containment, the tubes

$$\{t_i = \text{fill}_x(S_i) \mid i > k,\ t_i \in T\}$$

are all sequentially and properly contained inside of $t_k = \text{fill}_x(S_k)$. Indeed, they must be nested in the tubing since they intersect at least in x. Therefore, the tubes in S_k cannot all be found in $\mathfrak{S}_k$. If just some of the tubes of S_k are found in $\mathfrak{S}_k$, then the tubes of S_k that are not found in that collection cannot be in T, since they would be forced to intersect illegally with some of the t_i. And finally, the tubes of S_k cannot all reside in T since their union is not filled.

Therefore, since (5.1) does not contain S_k, truncating the face labeled by S_k will not separate the facets labeled by the tubes of $T_k - \{t_k\}$. However by our finite induction assumption, the face labeled by S_k does intersect the face where the facets labeled by $T_k - \{t_k\}$ intersect, so their intersection will further intersect the new facet labeled by t_k. Thus, the facets labeled by the tubes in T_k will have a nonempty intersection for each $k \in \{0, \ldots, m\}$. □

5.2. We now consider the second case in Theorem 6, when $\mathfrak{b}_x$ is non-singleton. By induction, the theorem holds for the poset formed by replacing $\mathfrak{b}_x$ with a singleton bundle $\{x\}$ that has the same boundary. That is, we can assume a poset isomorphism g between $\pi(P - (\mathfrak{b}_x - x))$ and $\mathcal{K}(P - (\mathfrak{b}_x - x))$.

Proposition 16. *For non-singleton $\mathfrak{b}_x$, there exists a poset isomorphism f from the poset of tubings $\pi(P)$ to the simple polytope $\mathcal{K}P$, found by truncating*

$$\mathcal{K}P_* \ := \ \mathcal{K}(P - (\mathfrak{b}_x - x)) \ \times \ \Delta_{|\mathfrak{b}_x - x|}\,,$$

as described in Section 3.

Proof. The facets of the truncated polytope $\mathcal{K}P$ are clearly in bijection with the tubes of P: tubes t that do not contain ∂x are present by induction and by the operation of cartesian product (in $\mathcal{K}P*$ they will be labeled by $(\{t\}, \mathfrak{b}_x)$ and so retain the label $\{t\}$ in $\mathcal{K}P$), whereas tubes that do contain ∂x will correspond to facets that are created via truncation.

Again, we show that f is an isomorphism of posets from $\pi(P)$ to $\mathcal{K}P$ by checking that facets $f(t)$ of $\mathcal{K}P$ intersect in a face $f(T)$ if and only if their respective tube labelings t form a tubing T of P. Since we are dealing with convex polytopes (where every set of facets intersects in a unique face, if at all), this simultaneously shows that f is a bijection of tubings and preserves the ordering of tubings.

Forward direction: Let T be a set of tubes that is not a tubing of poset P. We show the set of facets $\{f(t) \mid t \in T\}$ has empty intersection. Since P is connected, there is either

(1) a pairwise disjoint subset $S \subset T$ whose union is unfilled in P, or
(2) there is a pair of nonnested but intersecting tubes in T.

In the case of the former, when S is unfilled, we see implied a further subset S' that was unfilled in the poset $P-(\mathfrak{b}_x - x)$, where S' consists of the tubes of S with one modification: replacing any portion of $\mathfrak{b}_x$ in those tubes with x. Since, by induction, the facets labeled by tubes of S' have no common intersection in $\mathcal{K}(P-(\mathfrak{b}_x - x))$, and since the product of polytopes preserves this fact, then the faces of the product bearing labels from S' do not have a common intersection. Indeed, truncation cannot introduce an intersection that was not there before.[3]

Now consider when T contains intersecting, nonnested tubes, say t_1 and t_2 of P. Replace any portion of $\mathfrak{b}_x$ contained in them with x, resulting in

$$t_1' \;:=\; (t_1 - \mathfrak{b}_x) \;\cup\; \{x\} \quad \text{and} \quad t_2' \;:=\; (t_2 - \mathfrak{b}_x) \;\cup\; \{x\}\,.$$

If these tubes are still intersecting but nonnested, their facets in $\mathcal{K}(P-(\mathfrak{b}_x - x))$ had no intersection, and this property will be passed along to our new polytope.[4] However if the tubes t_1' and t_2' are nested or equal, then both t_1 and t_2 contained some of $\mathfrak{b}_x$, and we must further consider the intersection

$$t_1 \;\cap\; t_2 \;\cap\; \mathfrak{b}_x\,. \tag{5.2}$$

If this is empty, then $f(t_1)$ and $f(t_2)$ are facets created by truncating faces of $\mathcal{K}P_*$, which in turn corresponds to faces of $\Delta_{|\mathfrak{b}_x - x|}$ which did not intersect. Again, the non-intersection is inherited by $\mathcal{K}P$.[5]

Finally, if (5.2) is nonempty, then it is straightforward to see that the facets $f(t_1)$ and $f(t_2)$ result from truncating faces that originally intersect in $\mathcal{K}P_*$. Here, there is a third, prior truncation of a face f of $\mathcal{K}P_*$ that contains the intersection of the faces that are truncated to become $f(t_1)$ and $f(t_2)$. Indeed, the face f is labeled in $\mathcal{K}P_*$ by the smaller of t_1' and t_2', paired with (5.2). Thus, after truncation, it gives rise to the facet $f(t_1 \cap t_2)$. Therefore, it is truncated first and effectively separates the others, resulting in an empty intersection after their truncations.[6]

Backward direction: Let $\{t_1, \ldots, t_m\}$ be the tubes in P whose facets are formed via truncation. We use finite induction on this list to show that if T is a tubing of P, then $\{f(t) \mid t \in T\}$ has nonempty intersection. Our argument proceeds by constructing a series of $m+1$ sets of face labels that ends with the set T, and showing at each step that they do indeed label faces

[3]For Figures 11 and 12, $S = \{\{1\}, \{2, y\}\}$, giving rise to $S' = \{\{1\}, \{2, x\}\}$. The latter is not a face in $\mathcal{K}(P-(\mathfrak{b}_x - x))$ and the former labels disjoint facets in $\mathcal{K}P$.

[4]In Figures 11 and 12, tubes $t_1 = \{1, 2, a, y\}$ and $t_2 = \{1, 2, b, y\}$ label non-intersecting facets $f(t_1)$ and $f(t_2)$ in $\mathcal{K}P$ whereas tubes $t_1' = \{1, 2, a, x\}$ and $t_2' = \{1, 2, b, x\}$ label non-intersecting facets $g(t_1')$ and $g(t_2')$ in $\mathcal{K}(P-(\mathfrak{b}_x - x))$.

[5]In Figure 12, this is demonstrated by $t_1 = \{2, x\}$ and $t_2 = \{2, y\}$.

[6]In Figure 12, this is exemplified by $t_1 = \{1, 2, b, y\}$ and $t_2 = \{2, x, y\}$. The facets $f(t_1)$ and $f(t_2)$ are separated by the earlier truncation of the face of KP_* labeled by $(\{2, x\}, \{y\})$.

that intersect. For a tubing T of P, create the following set of labels of faces of $\mathcal{K}P_*$:

$$T_0 \;=\; \{\ (\ \{(t-\mathfrak{b}_x)\cup\{x\}\},\ t\cap\mathfrak{b}_x\ )\ \mid\ \partial x\subset t\in T\ \}\ \cup\ \{\ (\{t\},\ \mathfrak{b}_x)\ \mid\ \partial x\notin t\ \}.$$

This set gives a list of faces of $\mathcal{K}P_*$ whose intersection is nonempty, and furthermore, provides the base case for truncation due to the following reasons:

(1) Our construction of T_0 from T ensures that the first coordinates of the pairs in T_0 are tubes which constitute a tubing in $\mathcal{K}(P-(\mathfrak{b}_x-x))$. Thus, these tubes label a set of facets whose intersection is nonempty.
(2) Since T is a tubing, the tubes of T which contain ∂x are all nested. Thus, by our construction of T_0, the set of second coordinates of the pairs in T_0 are subsets of $\mathfrak{b}_x$ that have a common intersection, implying the faces they label in Δ_{k-1} also have a common nonempty intersection.
(3) Due to the lattice structure of the cartesian product of polytopes, the product $\mathcal{K}P_*$ of the two polytopes $\mathcal{K}(P-(\mathfrak{b}_x-x))$ and Δ_{k-1} will have the list of pairs labeling faces that also have a common nonempty intersection.

Now, recursively define an intermediate set of tubes called T_k, corresponding to having performed truncations to create the facets $f(t_1),\ldots,f(t_k)$. Let (s_k,B_k) be the label of the face truncated to make the facet t_k, implying that $s_k=(t_k-\mathfrak{b}_x)\cup\{x\}$. Given T_0 as described above, define T_k to be created from T_{k-1} as follows:

(1) If t_k is not in T, let $T_k=T_{k-1}$.
(2) Otherwise, T_k is formed by discarding from T_{k-1} the pair $(s_k,\,B_k)$ and replacing it with t_k itself (corresponding to labeling the new facet with the new tube t_k).

And for the last step, to make $T_{m+1}=T$, take T_m and replace any pairs $(\{t\},\mathfrak{b}_x)$ with $\{t\}$.

Example. From Figures 11 and 12, consider the tubing of P given by

$$T=\{\{1\},\{1,2,b,y\},\{1,2,b,x,y\}\}.$$

Here, we have

$$T_0=\{(\{1\},\{x,y\}),(\{1,2,b,x\},\{y\}),(\{1,2,b,x\},\{x,y\})\}.$$

The algorithm above first produces $T_0=T_1=T_2=T_3$, and then

$$T_4=T_5=T_6=T_7=\{(\{1\},\{x,y\}),\{1,2,b,y\},(\{1,2,b,x\},\{x,y\})\},$$

followed by

$$T_8=T_9=T_{10}=T_{11}=\{(\{1\},\{x,y\}),\{1,2,b,y\},\{1,2,b,x,y\}\},$$

and finally, $T_{12}=T$.

We assume that after truncating $k-1$ faces of $\mathcal{K}P_*$, the faces of the partly truncated polytope labeled with the elements of T_{k-1} have a nonempty common intersection. We show that after truncating the next face F_k on the list, labeled by (s_k, B_k), creating the facet $f(t_k)$, the faces labeled by the elements of T_k still have a nonempty intersection. We argue that F_k does not contain the face G_k, defined as the intersection of the set of faces labeled by the elements of $T_k - \{t_k\}$. Note that we only need to check this for $k < m$, since when $k = m$, we see $T_m - \{t_m\} = T_{m-1} - \{(s_m, B_m)\}$.

Note that t_k is either (1) contained in, or (2) intersects (but is not nested with) at least one tube in $\{t_{k+1}, \ldots, t_m\}$. In the latter case (2), $t_k \notin T$, and t_k either inherits an empty intersection with the faces represented by T_0 (from one of the two polytopes in the cross product), or is separated from the intersection of the faces represented by T_{k-1} by an earlier truncation (from the proof in the forward direction). Thus, F_k does not contain G_k.

Now consider the former case (1): When we truncate F_k, depending on the contents of t_k, we can describe a facet Y_k that contains F_k and none of the other faces labeled by the elements of $T_k - \{t_k\}$. Then F_k cannot contain G_k, and thus its truncation cannot separate the faces labeled by $T_k - \{t_k\}$. Specifically, if $B_k = B_{k+1}$, then Y_k is the facet labeled by $(s_k, \mathfrak{b}_x)$; if $B_k \subset B_{k+1}$, let Y_k be any facet labeled by $(P - (\mathfrak{b}_x - x), \mathfrak{b}_x - z)$, for a choice of some $z \in B_{k+1} - B_k$.

The facet originally labeled by the pair $(s_k, \mathfrak{b}_x)$, before any truncation, contains faces labeled by (s_k, B), for $B \subset \mathfrak{b}_x$. The facet labeled by the pair $(P - (\mathfrak{b}_x - x), \mathfrak{b}_x - z)$ contains faces labeled by (s, B), with $s \subset P - (\mathfrak{b}_x - x)$ and $B \subset \mathfrak{b}_x - z$. Thus, we have chosen Y_k to contain face F_k at step k, but none of the other faces scheduled to be truncated after it. Moreover, Y_k is chosen such that it will eventually be labeled by a tube t that intersects but is not nested with t_j, for $j > k$, and so t is not in T. Therefore, Y_k also cannot contain any of the facets forming the intersection G_k, both those labeled by tubes not containing ∂x and those created by earlier truncations.

Example. In Figures 11 and 12, let

$$T = \{\{2, y\}, \{1, 2, b, y\}, \{1, 2, b, x, y\}\}.$$

Then

$$T_0 = \{(\{2, x\}, \{y\}), (\{1, 2, b, x\}, \{y\}), (\{1, 2, b, x\}, \{x, y\})\}.$$

Next

$$T_1 = \{\{2, y\}, (\{1, 2, b, x\}, \{y\}), (\{1, 2, b, x\}, \{x, y\})\}.$$

The two faces represented by $T_1 - \{t_1\}$ intersect at this stage. Note that Y_1 is labeled by $(\{2, x\}, \{x, y\})$. Continuing the algorithm, we see $T_2 = T_1$ since $t_2 = \{2, x\} \notin T$. (Note that the order of t_1 and t_2 is arbitrary since they both have cardinality two.) However, the truncation

of F_2 labeled by $(\{2,x\},\{x\})$ does not separate the faces labeled by T_2 since F_2 does not contain their intersection G_2, due to an empty intersection inherited from the simplex in the product producing $\mathcal{K}P_*$.

Next $T_3 = T_2$, since $t_3 = \{2,x,y\} \notin T$. This truncation also leaves intact the intersection, since F_3 was separated from G_3 when we truncated to create $f(t_1)$. Next,

$$T_4 = \{\{2,y\},\{1,2,b,y\},(\{1,2,b,x\},\{x,y\})\}.$$

Here, we must use the facet Y_4 labeled by $(\{1,2,a,b,x\},\{y\})$, since the only z in $B_{k+1} - B_k = \{x,y\} - \{y\}$ is $z = x$, leaving us with $\mathfrak{b}_x - z = \{y\}$. Note that Y_4 does contain F_4 but not G_4, and of course we see that F_4 does not contain G_4, so that the faces labeled by $T_4 - \{t_4\}$ do have nonempty intersection. The reader can continue the process to reach $T_{12} = T$.

Finally, note that the truncated face labeled by (s_k, B_k) was guaranteed (by the finite induction assumption) to non-trivially intersect the common intersection of all the other faces represented by T_{k-1}. Therefore, the faces represented by T_k have a common intersection for $k \leq m$, and thus the tubing $T = T_{m+1}$ (formed just by renaming some facet labels in T_m) will be represented by facets with a common intersection in $\mathcal{K}P$. □

Acknowledgments. We are thankful to Federico Ardila, Vic Reiner, and Lauren Williams for their encouragement, and to the referees for valuable corrections and comments.

References

1. J. Bloom. A link surgery spectral sequence in monopole Floer homology, *Advances in Mathematics* **226** (2011) 3216–3281.
2. V. Buchstaber and V. Volodin. Combinatorial 2-truncated cubes and applications, in *Associahedra, Tamari Lattices and Related Structures*, Progress in Mathematics **299** (2013) 161–186.
3. M. Carr and S. Devadoss. Coxeter complexes and graph associahedra, *Topology and its Applications* **153** (2006) 2155–2168.
4. M. Carr, S. Devadoss, S. Forcey. Pseudograph associahedra, *Journal of Combinatorial Theory, Series A* **118** (2011) 2035–2055.
5. M. Davis, T. Januszkiewicz, R. Scott. Fundamental groups of blow-ups, *Advances in Mathematics* **177** (2003) 115–179.
6. C. De Concini and C. Procesi. Wonderful models of subspace arrangements, *Selecta Mathematica* **1** (1995) 459–494.
7. S. Devadoss. Tessellations of moduli spaces and the mosaic operad, in *Homotopy Invariant Algebraic Structures*, Contemporary Mathematics **239** (1999) 91–114.
8. S. Devadoss. A realization of graph associahedra, *Discrete Mathematics* **309** (2009) 271–276.
9. K. Došen and Z. Petrić. Hypergraph polytopes, *Topology and its Applications* **158** (2011) 1405–1444.
10. E. Feichtner and B. Sturmfels. Matroid polytopes, nested sets and Bergman fans, *Portugaliae Mathematica* **62** (2005) 437–468.

11. S. Forcey and D. Springfield. Geometric combinatorial algebras: cyclohedron and simplex, *Journal of Algebraic Combinatorics* **32** (2010) 597–627.
12. J. Morton, L. Pachter, A. Shiu, B. Sturmfels, O. Wienand. Convex rank tests and semigraphoids, *SIAM Journal on Discrete Mathematics* **23** (2009) 1117–1134.
13. Z. Petrić. On stretching the interval simplex-permutohedron, *Journal of Algebraic Combinatorics* **39** (2014) 99–125.
14. A. Postnikov. Permutohedra, associahedra, and beyond, *International Mathematics Research Notices* **6** (2009) 1026–1106.
15. S. Saneblidze and R. Umble. Diagonals on the permutohedra, multiplihedra and associahedra, *Homology, Homotopy and Applications* **6** (2004) 363–411.
16. J. Stasheff. Homotopy associativity of H-spaces, *Transactions of the American Mathematical Society* **108** (1963) 275–292.
17. W. Stein et al. *Sage Mathematics Software*, The Sage Development Team, 2014.
18. A. Zelevinsky. Nested complexes and their polyhedral realizations, *Pure and Applied Mathematics Quarterly* **2** (2006) 655–671.
19. Calculations available at `http://math.uakron.edu/~sf34/`

S. Devadoss: Williams College, Williamstown, MA 01267
E-mail address: `satyan.devadoss@williams.edu`

S. Forcey: University of Akron, OH 44325
E-mail address: `sf34@uakron.edu`

S. Reisdorf: University of Akron, OH 44325
E-mail address: `stephenreisdorf@gmail.com`

P. Showers: University of Akron, OH 44325
E-mail address: `pjs36@zips.uakron.edu`